Catalysis Today 147S (2009) S144–S148

Contents lists available at ScienceDirect

Catalysis Today

journal homepage: www.elsevier.com/locate/cattod

Supported ionic liquid catalysts—From batch to continuous operation in preparation of fine chemicals

Pasi Virtanen [a], Jyri-Pekka Mikkola [a,b], Esa Toukoniitty [a], Hannu Karhu [c], Krisztian Kordas [d], Kari Eränen [a], Johan Wärnå [a], Tapio Salmi [a,*]

[a] Åbo Akademi, Process Chemistry Centre, Laboratory of Industrial Chemistry and Reaction Engineering, FI-20500 Turku/Åbo, Finland
[b] Department of Chemistry, Technical Chemistry, Chemical Biological Centre, Umeå University, Umeå, Sweden
[c] Department of Applied Physics, University of Turku, FIN-20014 Turku, Finland
[d] Microelectronics and Materials Physics Laboratories, University of Oulu, FIN-90570 Oulu, Finland

ARTICLE INFO

Article history:
Available online 3 August 2009

Keywords:
Catalysis
Catalyst support
Continuous structured reactor ionic liquid
Multiphase reactions
Supported ionic liquid catalyst (SILCA)

ABSTRACT

The use of ionic liquids in catalysis is attracting ever more attention in chemical engineering. In line with this research we have studied supported ionic liquid catalysts (SILCAs) which consist of immobilized catalytic species, e.g., transition metal particles residing in an ionic liquid layer immobilized on a solid support, in batch mode operations. In this study the same concept was successfully applied in continuous mode applying a three-phase structured reactor in the hydrogenation of citral.

© 2009 Elsevier B.V. All rights reserved.

1. Introduction

Ionic liquids are completely ionic compounds, meaning that they are formed only of ionic species, cations and anions. Typically ionic liquids are formulated as a combination of a large organic cation with the possibility of charge delocalization and, consequently, a relatively large inorganic or organic anion. They have many exceptional properties compared to conventional ionic compounds. The main difference is their significantly lower melting point. For example, sodium chloride has a melting point of 801 °C, whereas many ionic liquids have a melting point below room temperature. Other special characteristic features that can be attributed to most of them are often a negligible vapor pressure ($\sim 10^{-8}$ bar), they are liquid over a wide temperature range, they have unique solvation properties, meaning that a wide variety of polar and non-polar compounds are soluble in ionic liquids, they have a wide electrochemical window and a good ion conductivity [1–3]. It should be kept in mind that these features are not common to every single ionic liquid, as has recently been stated by Deetlefs and Seddon [4]. Even if ionic liquids have shown their abilities in various chemical applications [5], a widespread use of ionic liquids in industrial applications is still hampered by the cost aspects, limited knowledge of their physical and chemical properties as well as concerns about their biodegradability.

The research in the field of ionic liquids is continuously attracting more interest in the scientific world. Many new applications and improved techniques have already been introduced, such as Basil® process by BASF, Difasol process by IFP and alkylation of isobutene by PetroChina [5]. Catalysis is one of the areas, where ionic liquids have already shown their potential in enhancing the reaction rates of many reactions [6–8].

Utilizing the special characteristics of ionic liquids by immobilizing small amounts of them on solid surfaces is an attractive alternative [9]. In fact, catalysis is one of the areas, where this concept has already been utilized [10–15]. Supported ionic liquid catalysts (SILCA) are special kinds of catalysts which were developed at the beginning of this millennium. SILCA consists of three different parts. First, there is a porous solid support material. The support material can be, for example, alumina, silica or active carbon, *i.e.*, a typical catalyst support material. The second part of the system is a thin layer of ionic liquid. Ionic liquid is thus immobilized on the support material. Immobilization can be achieved simply by physisorption or one of the ions can be chemically bonded to the support. The third part is the catalyst itself, in the form of catalytically active metal nanoparticles or metal complexes, which are dissolved in the ionic liquid layer. A catalyst which contains palladium nanoparticles in the ionic liquid layer, which in turn is immobilized on active carbon, is presented in Fig. 1. This kind of catalyst was used in the present work.

---

[*] Corresponding author.
E-mail address: tsalmi@abo.fi (T. Salmi).

0920-5861/$ – see front matter © 2009 Elsevier B.V. All rights reserved.
doi:10.1016/j.cattod.2009.07.020

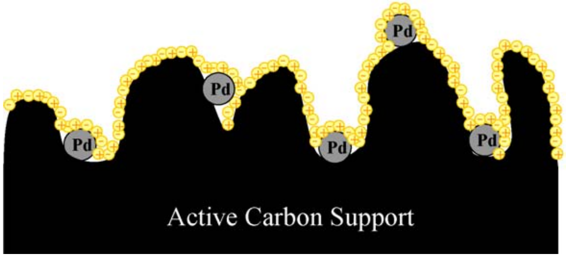

Fig. 1. A supported ionic liquid catalyst (SILCA) used in hydrogenation. The black area represents the active carbon support, while the yellow spots are the cations and anions of the ionic liquid and the grey circles are the palladium nanoparticles. (For interpretation of the references to color in this figure legend, the reader is referred to the web version of the article.).

Selective hydrogenation of α,β-unsaturated aldehydes, ketones and esters, in general, is a versatile pathway to obtain many interesting products which can be used in perfumes, hardening of fats, preparation of pharmaceuticals and synthesis of organic intermediates. Citral itself and its hydrogenation products are widely used in perfumery and fine chemical industries. Selective hydrogenations of α,β-unsaturated aldehydes and ketones are challenging, because these species contain three chemically different double bonds: isolated and conjugated carbon–carbon double bonds as well as a carbonyl group. Consequently, during the hydrogenation of citral, competing and consecutive reactions can take place, including formation of ring compounds, such as pulegols and menthols. These kinds of reactions have been widely studied on conventional heterogeneous and homogeneous catalysts in conventional as well as supercritical solvents and ionic liquids [16–22]. SILCA has already shown its capability in hydrogenation of alkenes, compared to biphasic systems and conventional solvents [14,23]. During this work, the hydrogenation of slightly more complex compound, namely citral was studied over SILCA.

This study continues our previous work where we applied these kinds of catalysts in hydrogenation of citral in a batch reactor [22,24–26]. The same kind of catalyst was now applied in hydrogenation of citral in a continuously operated structural three-phase reactor.

2. Experimental

2.1. Catalyst preparation

A straightforward catalyst preparation method was applied [26]. Palladium acetylacetonate ($Pd(acac)_2$) (approximately 50 mg) (Aldrich 99%) and an ionic liquid, *N*-butyl-4-methylpyridinium tetrafluoroborate ($[NB4MPy][BF_4]$, Merck, 98%) (approximately 150 mg) were dissolved in acetone (Merck, p.a.). The solution was poured over Active Carbon Cloth (ACC Kynol®, approximately 1200 mg). ACC was dried a priori at 60 °C over 12 h. The wetted catalyst was kept in an oven, at 80 °C, for 2 h until all acetone was evaporated and cut into circular pieces with diameter of 9 mm.

2.2. Testing activity and selectivity of the catalyst

The catalyst was applied in the hydrogenation of citral (Lancaster, 95%). Experiments were performed in a tubular stainless steel reactor ($V_L = 1{,}3\ cm^3$, i.d. = 9 mm, $h = 145$ mm,) where the catalyst cloths were packed in layer by layer on a stainless steel net in order to immobilize the catalyst. A small amount of quartz wool was set on top of the catalyst layers to distribute the flows evenly over the catalyst. The reactor was equipped with a heating jacket and a thermocouple just below the catalyst bed in order to keep the temperature constant during the experiments. The catalyst was pretreated *in-situ* prior the experiment at 120 °C under hydrogen flow of 5 bar. As a result, a catalyst containing palladium nanoparticles in an ionic liquid, immobilized on ACC was achieved. Citral (approximately 4.3 g) was dissolved in 350 ml of *n*-hexane (Merck, pro analysis). The solution was saturated with hydrogen in a separate vessel before it was pumped to the reactor. Hydrogen ($\sim$50 $cm^3\ min^{-1}$) and the liquid phase ($\sim$2 $cm^3\ min^{-1}$) were flowing co-currently through the reactor. The reactor system is illustrated in Fig. 2.

In order to evaluate the performance of the catalyst samples were withdrawn after the reactor and analyzed by gas chromatography (Hewlett Packard 6890 GC with an FI detector). 500 μl of internal standard (0.02 M cyclohexanone in cyclohexane) was added into a 500 μl of the sample. The column in the system was an Agilent DB-1 with a length of 30 m, inner diameter of 0.25 mm and, the film thickness of 0.5 μm. The samples were analyzed with the following temperature program: temperature was at first held 10 min at 100 °C, then raised 5 °C/min to 160 °C, and consequently held 10 min at 160 °C, followed by a temperature ramp 13 °C/min to 200 °C, and was held 1 min at 200 °C.

2.3. Catalyst characterization

The catalyst was characterized as fresh after the pre-treatment procedure before it was applied in hydrogenation experiment.

The binding energies of all the compounds and oxidation state of Pd on the ACC-support were determined by investigating the catalysts by means of X-ray photoelectron spectroscopy (XPS). A PerkinElmer PHI 5400 spectrometer was applied with Mg Kα radiation (1253.6 eV) and a pass energy of 35.75 eV. The pressure during the analysis was ca. 8×10^{-9} mbar. The reduced sample was stored in a nitrogen atmosphere after the pre-treatment process. However, during the transfer to the XPS instrument, the sample was in contact with ambient air and it was out-gassed overnight. The ionic liquid partially evaporated during out-gassing under the ultrahigh vacuum conditions. Hence, boron and fluorine, which have relatively low photoionization cross-sections, were in some conditions below the detection limit. The observations are largely based on residual ionic liquid in the pores of the active

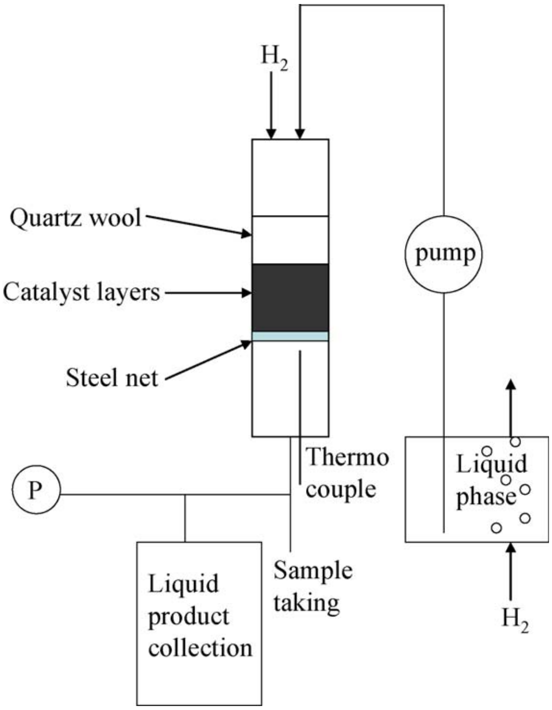

Fig. 2. A schematic picture of the reactor system applied in this study.

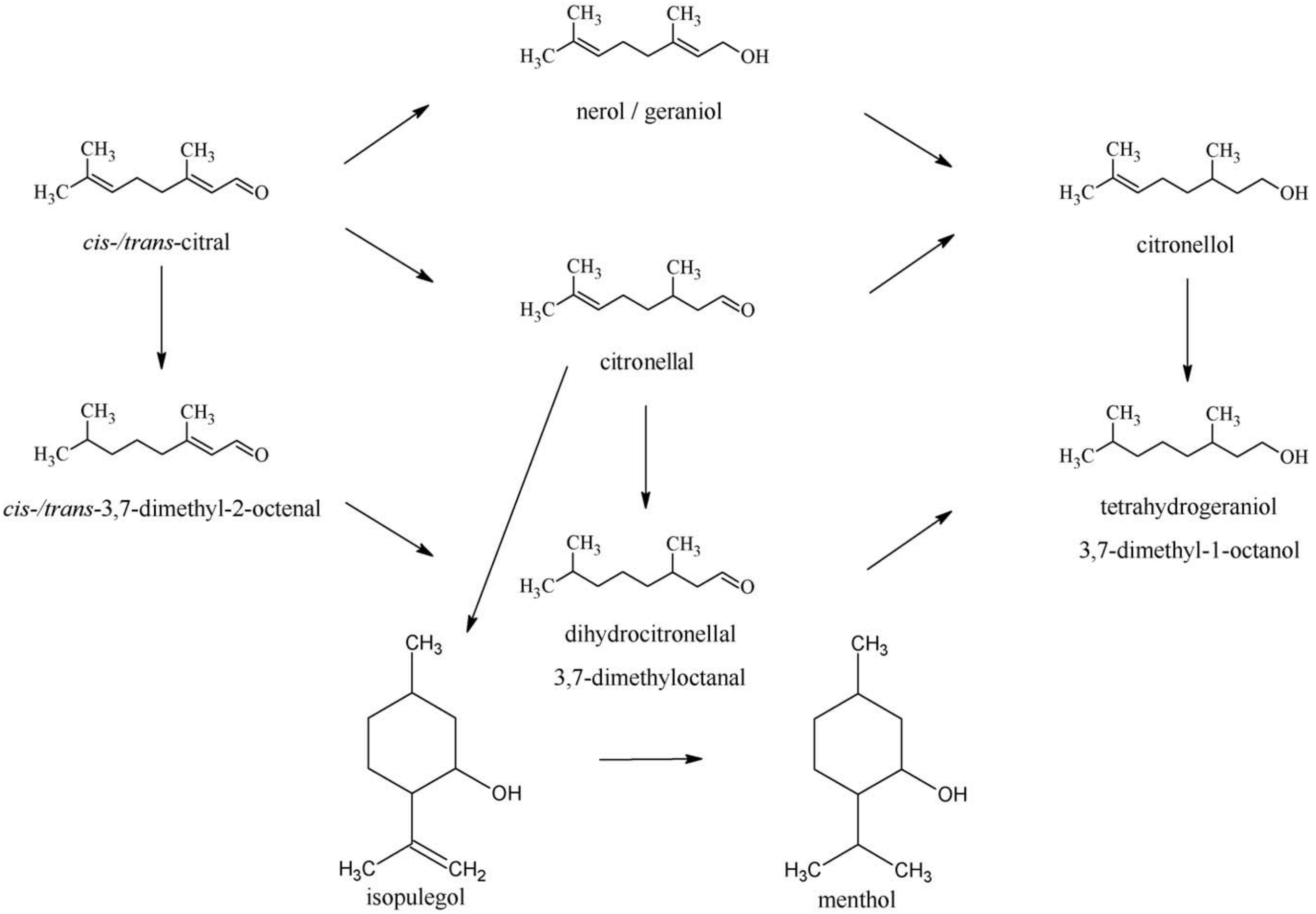

Scheme 1. Citral hydrogenation reaction sequence.

carbon cloth. The binding energies (BEs) were determined by line fitting procedure, where the line shape of the fitted peaks was a convolution of a Doniach-Šunjić line shape with a Gaussian line shape. A linear background was used for the signal background subtraction. The accuracy of the binding energies was ±0.1 eV. In the quantitative analysis, the sensitivity factors for B 1s and F 1s were 0.159 and 1.000. In the case of palladium, Pd $3d_{5/2}$ and $3d_{3/2}$ intensity ratios were kept fixed at 3:2 and a mixture of Gaussian and Lorentzian line shapes was used. Carbon 1s line at 284.7 eV was used as an energy reference in correcting the binding energy axis for a minor sample charging under the X-ray bombardment.

The catalyst was also investigated by means of energy-filtered transmission electron microscopy (EFTEM LEO 912 OMEGA), equipped with an energy dispersive X-ray detector. For the EFTEM analyses, the sample was crushed and dispersed in *n*-hexane before dispensing them on the specimen holder copper grid (formvar/carbon).

The surface area and micro-pore volume of the catalyst was determined by an automatic physisorption–chemisorption apparatus (Carlo Erba instruments, sorptometer 1900). Dubinin method was used to calculate surface area of catalysts from the measurement data. Dollim/Heal method was used to determine micro-pore volume of catalyst.

3. Results and discussion

3.1. Catalyst activity and selectivity

Hydrogenation of citral over SILCA catalyst was performed in a plug flow reactor applying continuous hydrogen flow as well as liquid flow in a co-current mode. The reaction was performed at different temperatures and hydrogen pressures. During the hydrogenation of citral, a number of competing and consecutive reactions can take place. The reaction network for the main transformations is presented in Scheme 1. Other minor products formed and identified during the experiments were different alkanes and alkenes formed by dehydration and cracking.

The activity of the catalyst in different conditions can be evaluated when the amount of citral hydrogenated during the experiment is compared. In Fig. 3, the amount of citral hydrogenated is calculated per amount of palladium used during unit time, in order to eliminate small variations in the catalyst loading and liquid flow.

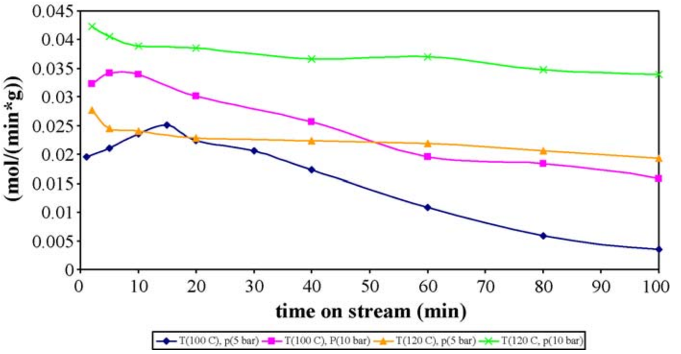

Fig. 3. Comparison of catalyst activity in different temperatures. In figure, the amount of citral hydrogenated per used amount of palladium per time unit is presented during the experiments in different temperature and pressure.

Fig. 3 shows that the reaction temperature has a strong influence on the catalyst activity. The activity decline was severe at 100 °C, whereas only modest catalyst deactivation took place at 120 °C. It can be seen that at lower temperature, the activity of the catalyst has some kind of induction or activation period in the beginning of the experiments followed by a rather rapid deactivation. With slightly higher temperature this induction period is totally missing and the deactivation is also much slower. Explanation for these both phenomena can simply be adsorption of the polar compounds in the ionic liquid layer. At lower temperature it takes longer time to reach the adsorption/desorption equilibrium for the reactants and products. On the other hand, the rapid deactivation can be caused by accumulation of polar hydrogenation products as was also the case in batch hydrogenation of citral [24]. Same phenomenon has also been reported in hydroformylation reaction with similar type of catalyst [27]. Apparently, at higher temperature this adsorption/desorption equilibrium is reached quickly and also the accumulation of polar products to the ionic liquid layer is not so rapid. Also, the presence of hydrogen helps to reactivate the catalyst by hydrogenating away the carbonaceous residues. The reactivation rate is higher at higher temperatures, which might explain the slower activity decline at higher temperature. The selectivity of different hydrogenation products was somewhat as expected since palladium is known to promote the hydrogenation of carbon–carbon double bond instead of carbonyl group. However, the selectivity of different hydrogenation products was clearly varied in different conditions (Fig. 4.). When hydrogen pressure is higher at both temperatures the selectivity of 3,7-dimethyloctanal increases which is expected since 3,7-dimethyloctanal is more hydrogenated product of citral (Scheme 1) and produced more when more hydrogen is available. The lower selectivity of 3,7-dimethyloctanal at higher temperature can be explained by adsorption/desorption equilibrium of citronellal and 3,7-dimethyl-2-octrnal. At higher temperature they are not so strongly adsorbed on the palladium particles and does not give a possibility the reaction to go further to 3,7-dimethyloctanal. The selectivities were somewhat different than with same catalyst in batch process where 3,7-dimethyloctanal was clearly the main product at all conditions [24]. This can be explained by longer time that the reactants were in contact with the catalyst, thus selectivities of citronellal 3,7-dimethyloctanal and 3,7-dimethyl-2-octenal could be altered by adjusting the liquid flow or the concentration of citral feed in continuous process.

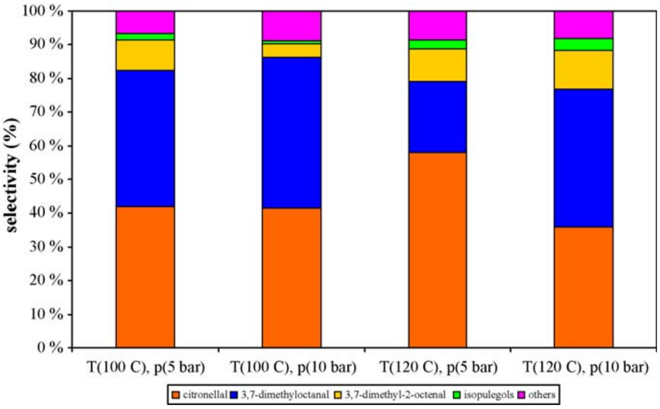

Fig. 4. Comparison of the selectivities of the citral hydrogenation products under different conditions at the end of the experiments (*t* = 100 min). Other compounds are reaction products from dehydration and cracking of citral and its hydrogenation products.

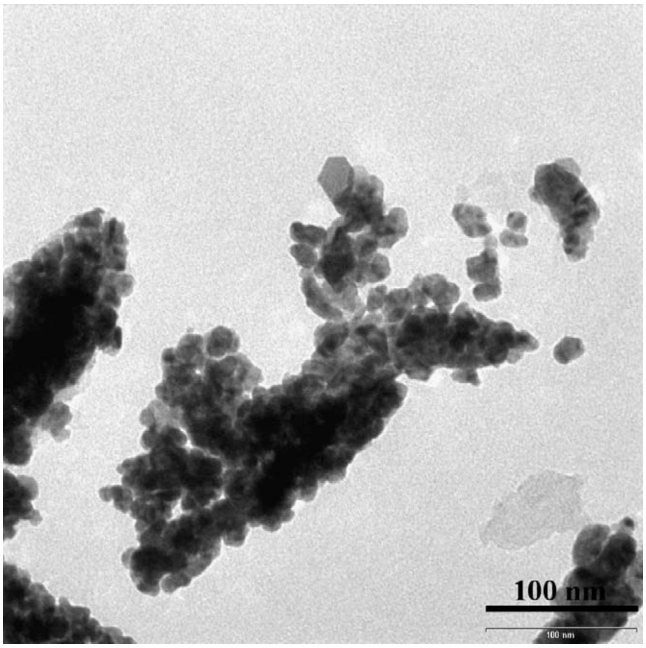

Fig. 5. EFTEM picture of the supported ionic liquid catalyst containing palladium particles (black spots and areas) in *N*-butyl-4-methylpyridinium tetrafluoroborate on ACC.

3.2. Catalyst characterization

Results from the XPS analysis showed that the observed Pd $3d_{5/2}$ binding energy (ca. 335.5 eV) is slightly above the bulk metal (335.1 eV) [28], which indicates that Pd metal particles were formed during the catalyst pre-treatment process.

FESEM and EFTEM analysis of the catalysts proved that Pd nanoparticles were formed during catalyst pre-treatment. However, also some agglomerated Pd particles were formed. A picture of the catalyst is presented in Fig. 5.

The result of nitrogen physisorption measurement of the fresh catalyst gave 1400 m^2/g for the specific surface area (Dubinin) and 0.5 cm^3/g for the micro-pore volume (Dollim/Heal) and 400 m^2/g and 0.1 cm^3/g for the spent catalyst respectively. The specific surface area of pure ACC is 1680 m^2/g and micro-pore volume 0.6 cm^3/g. The amount of ionic liquids was approximately 0.15 g and $Pd(acac)_2$ 0.05 g. The total amount of Pd metal was only 0.017 g or 1.6×10^{-4} mol. The amount of ACC-support used for a single catalyst was approximately 1.2 g. Thus, the Pd content of the catalysts was only about 1 wt.%. The density of *N*-butyl-4-methylpyridinium tetrafluoroborate, the ionic liquids used in this study, is, at ambient conditions, 1.18 g/cm^3 [29]. Thus, it can be estimated that 20–30 vol.% of the pore volumes were filled with an ionic liquid layer. The smaller surface area and micro-pore volume of the spent catalysts indicate the adsorption of carbonaceous residues on the on the catalyst as discussed above. Consequently, this is presumably the primary reason for the catalyst deactivation.

4. Conclusions

The goal of this study was to demonstrate that supported ionic liquid catalysts (SILCA) can successfully be employed also in a continuous hydrogenation processes by using the structured catalyst concept (SILCA on layers of active carbon cloth). Our earlier studies showed that the catalysts could be used in batch hydrogenation process. However, the results in this study showed that also continuous hydrogenation process can be applied. We were able to prepare, characterize and use the catalysts in the hydrogenation of citral. This reaction merely represents an example of possible sample cases. The characterization results verified that active metal (palladium) nanoparticles were formed on the catalyst support during the catalyst pre-treatment process.

Acknowledgments

The financial support from the Academy of Finland is gratefully acknowledged (Decisions nr. 124640, 209391 and 211463). This work is a part of the activities at the Åbo Akademi Process Chemistry Centre (PCC) within the Finnish Centre of Excellence Programmes (2000–2005 and 2006–2011) by the Academy of Finland.

References

[1] P. Bonhôte, A.-P. Dias, N. Papageorgiou, K. Kalyanasundaram, M. Grätzel, Inorg. Chem. 35 (1996) 1168.
[2] R.D. Rogers, K.R. Seddon, Science 302 (2003) 792.
[3] K.R. Seddon, Nat. Mater. 2 (2003) 363.
[4] M. Deetlefs, K.R. Seddon, Chim. oggi – Chem. Tod. 24 (2006) 16.
[5] N.V. Plechkova, K.R. Seddon, Chem. Soc. Rev. 37 (2006) 123–150, 2008.
[6] J. Dupont, G.S. Fonseca, A.P. Umpierre, P.F.P. Fichtner, S.R. Teixeira, J. Am. Chem. Soc. 124 (2002) 4228.
[7] R. Sheldon, Chem. Commun. (2001) 2399.
[8] C.M. Gordon, App. Catal. 222 (2001) 101.
[9] M.H. Valkenberg, C. deCastro, W.F. Hölderich, Green Chem. 4 (2001) 88, 2002.
[10] S. Breitenlechner, M. Fleck, T.E. Mueller, Suppan, J. Mol. Catal. A 214 (2004) 175.
[11] D.W. Kim, D.Y. Chi, Angew. Chem. Int. Ed. 43 (2004) 483.
[12] A. Riisager, R. Fehrmann, S. Flicker, R. van Hal, M. Haumann, P. Wasserscheid, Angew. Chem. Int. Ed. 44 (2005) 815.
[13] H. Hagiwara, Y. Sugawara, K. Isobe, T. Hoshi, T. Suzuki, Org. Lett. 6 (2004) 2325.
[14] J. Huang, T. Jiang, H. Gao, B. Han, Z. Liu, W. Wu, Y. Chang, G. Zhao, Angew. Chem. Int. Ed. 43 (2004) 1397.
[15] C.P. Mehnert, Chem. Eur. J. 11 (2005) 50.
[16] P. Claus, Top. Catal. 5 (1998) 51.
[17] G. Neri, L. Mercadante, A. Donato, A.M. Visco, S. Galvagno, Catal. Lett. 29 (1994) 379.
[18] P. Gallezot, A. Giroir-Fendler, D. Richard, Catal. Lett. 5 (1990) 169.
[19] F. Joó, J. Kovács, A.C. Bényei, Á. Kathó, Catal. Tod. 42 (1998) 441.
[20] M. Burgener, R. Furrer, T. Mallat, Baiker, Appl. Catal. A: Gen. 268 (2004) 1.
[21] K. Anderson, P. Goodrich, C. Hardacre, D.W. Rooney, Green Chem. 5 (2004) 448.
[22] P. Virtanen, H. Karhu, G. Toth, K. Kordas, J.-P. Mikkola, J. Catal. 263 (2009) 209.
[23] C.P. Mehnert, E.J. Mozeleski, R.A. Cook, Chem. Commun. 2002 (2004) 3010–3011.
[24] P. Virtanen, H. Karhu, K. Kordas, J.-P. Mikkola, Chem. Eng. Sci. 62 (2007) 3660.
[25] P. Virtanen, J.-P. Mikkola, T. Salmi, Ind. Eng. Chem. Res. 46 (2007) 9022.
[26] J.-P. Mikkola, P. Virtanen, H. Karhu, T. Salmi, D.Y. Murzin, Green Chem. 8 (2006) 197.
[27] A. Riisager, R. Fehrmann, M. Haumann, B.S.K. Gorle, P. Wasserscheid, Ind. Eng. Chem. Res. 44 (2005) 9853.
[28] J.F. Moulder, W.F. Stickle, P.E. Sobol, K.D. Bomben, Handbook of X-ray Photoelectron Spectroscopy, PerkinElmer Corp., Physical Electronics Division, USA, 1992.
[29] A. Heintz, D.V. Kulikov, S.P. Verevkin, J. Chem. Eng. Data 46 (2001) 1526.